In pursuit of propulsion at the nanoscale†

Stephen J. Ebbens and Jonathan R. Howse*

Received 8th September 2009, Accepted 26th November 2009
First published as an Advance Article on the web 15th January 2010
DOI: 10.1039/b918598d

This review describes recent developments in self-propelling nano- and micro-scale swimming devices. The ability of these devices to transport nano-scale components in a fluidic environment is demonstrated. Furthermore, the adaptations needed for these devices to meet biological transport challenges such as targeted drug delivery are highlighted. Particular emphasis is placed on describing autonomously powered devices driven by asymmetrical chemical reactions. Methods to control the speed and direction of such swimming devices using external fields are described, and contrasted to recent demonstrations of statistical autonomous migrations and organisations driven by chemical gradients, inter swimmer interactions and external photo-stimulus. Finally the challenges and advantages of converting other nature inspired swimming mechanisms into realistic artificial self-powered devices are considered.

1. Introduction

Many of the currently proposed nanotechnologies present significant transport challenges if they are to fulfil their envisaged applications. For example, how will individual nanoscale-components be moved and organised to form complete machines? Also, how will drug laden nanoparticle pay-loads be delivered to specific cellular targets? Recently significant advances have been made in the development of nanoscale and microscale swimming devices that possess the potential to address these goals.[1] Such devices can now be made to locate, pick-up and deposit micron scale cargo, and autonomously accumulate in response to a chemical signal. In this context, the capabilities of existing nano- and micro scale swimming devices are described here to measure progress in this field and suggest future directions.

As it seems likely that nano-scale components will be transported using equivalently sized devices, this review focuses on translators with dimensions ranging from hundreds of nanometres to tens of microns, a common size range for useful nanotechnology components. Considering fluid behaviour on these length scales it is apparent that a number of challenges are posed. Principal amongst these is the well known absence of inertial effects at the low Reynolds numbers applicable to miniature devices in aqueous solutions. This rules out propulsion driven by conventional swimming mechanisms that rely on gliding between time-reversible movements, as famously visualised by a single hinged miniature "scallop" achieving no net progress by symmetrically flapping its' arms.[2] Another key factor at these length scales is the dominance and ubiquity of Brownian motion. Of particular note is the rapid rotation imparted to symmetrical micron scale objects, making the generation of

Department of Chemical and Process Engineering, University of Sheffield, Sheffield, S1 3JD, UK. E-mail: j.r.howse@sheffield.ac.uk; Fax: +44 (0) 114 2227501; Tel: +44 (0) 1142227596

† This paper is part of a *Soft Matter* themed issue on Emerging Themes in Soft Matter: Responsive and Active Soft Materials. Guest Editors: Anna C. Balazs and Julia Yeomans.

Stephen J. Ebbens

Stephen Ebbens obtained his PhD investigating the surface properties of polymers at Durham University in 2000. Since then he worked in industry developing techniques to characterise pharmaceutical devices, before developing an ink-jet printing method for self-assembled monolayers at Loughborough University. Stephen moved to Sheffield University in 2008 and is currently developing and characterising novel swimming devices in the Department of Chemical and Process Engineering.

Jonathan R. Howse

Jonathan Howse obtained his PhD in 2000 (Sheffield) investigating critical phenomena in binary liquid mixtures using neutron and X-ray reflectivity. Following a 2 year research position at the Berlin Neutron Scattering Centre and the TU-Berlin he returned to Sheffield to conduct research on a variety of "soft-nanotechnology" projects with Prof. Tony Ryan and Prof. Richard Jones. He was appointed lecturer in 2007.

constant, directed motion impossible without developing suitable steering mechanisms to maintain orientation or by applying an external bias. It is for this reason that nature often solves nano-scale transport problems by confining objects to tracks overcoming such perturbations.[3,4]

To address these identified transport challenges it is apparent that small scale swimming transporters should ideally operate autonomously without the need for external guidance or power. Indeed for many biological applications this requirement will be essential, due to the impracticality of providing external steering or powering fields, and tracking the location of the devices as they operate. For nano-assembly applications carried out in more agreeable environments there is a greater flexibility to apply external fields and monitor device location, however the principle of keeping external interventions to a minimum will result in more efficient, reliable, high throughput processes.

Considering these restrictions it is maybe less surprising that the number of potential swimming mechanisms for transporters on these length scales is limited. Nature uses rotating or wave propagating flagella to effect movement of micron scale bacteria and other cells, but at present all artificial mimics require external power sources. In addition, although theoreticians have proposed numerous model swimmers[5] that overcome low Reynolds number issues these have not yet been realised without external manipulations, due to both the lack of a suitable power source and the complexity of the required mechanical movements.

In fact, this difficulty in powering "moving-part" swimmers, and other devices, at small scales is one of the key challenges in nano-technology at present. Power generating systems used to produce movement at larger scales are usually heat engines, relying on temperature gradients to transfer energy to a liquid or gas that consequently undergoes expansion. However such heat engines fail at the nanoscale as maintaining the required temperature differential becomes impossible.[6] Attempts at miniaturising the pipes, pistons, seals, and other moving parts required by heat engine designs to scales approaching those demanded has proved to be difficult, and many fabricated prototypes have displayed low efficiency.[7] Furthermore, the large temperature differences necessary for heat engines to function are incompatible with biological systems, and would result in unwanted convection currents in assembly type applications.

As a result of these limitations, it is instructive to consider the functioning nanotechnology associated with cell biology. It should be noted that such systems are isothermal, far removed from heat engines, and instead powered by chemical potential. Indeed this approach is used to power biological motors where the hydrolysis of bio molecules such as adenosine triphosphate (ATP) is commonly used as an energy source. This results in small conformational changes in attached molecules that are amplified by complex molecular structures, and diffusive effects, to ultimately result in linear motion or translation. It is therefore a much more attractive strategy for synthetic devices, at these smaller length scales, to use the energy released from chemical reactions to generate motion.

Further analysis of biological swimming apparatus reveals that asymmetry is also vital to generate motion in a consistent direction, for example translating biological motors such as kinesin rely on the structural asymmetry of their filaments to produce uni-directional movement, and at larger scales flagella undergo asymmetric deformations.

This review focuses on a class of self-motile devices based on combining the concepts of autonomous chemical power generation and asymmetry; those driven by asymmetrical catalytic reactions. This class of swimmers operates according to the general principle of using localised catalytic decomposition of a dissolved fuel to generate an asymmetry at their surface or in their interfacial region, which in turn results in propulsion. Despite sharing a similar morphology, these swimmers exhibit a range of different propulsion mechanisms, the understanding of which is likely to prove key in future developments. In general the success of these "swimmers" relies on their ability to directly generate propulsion from a chemical reaction. This is in contrast to other mechanisms which require chemical energy to be converted into expansions and contractions, a task which can only be synthetically achieved currently with low efficiency, at larger scales and longer time scales than those required.

The first demonstration of the concept of swimming powered by asymmetrical chemical reactions can be traced back to work by Whitesides and co-workers who made millimetre scale chemically powered surface swimmers, Table 1, A1.[8] Since then, micron and nano-scale asymmetric chemically powered swimmers have been divided into conductive and non-conductive categories. While the pioneering demonstration of micro-swimming occurred in 2004 when Paxton *et al.*[9] and Fournier-Bidoz *et al.*[10] reported the propulsion of conducting nano-rod devices, this review initially discusses a later developed non-conducting swimmer to provide a more straightforward introduction to propulsion mechanisms, before returning to the more complex case of conductive devices. Nature inspired artificial flagella and other theoretical mechanistic suggestions are finally briefly described to allow mechanistic comparison with the autonomous translators.

2. Self-motile propulsive particles

2.1 Self-diffusiophoretic swimmers

Phoretic transport is the general term used to describe colloidal drift effects caused by external fields interacting with the interfacial boundary region of individual particles.[11] For example, electrophoretic colloidal movement results from an applied electric field causing a charged particle's diffuse counter ion cloud to move in the opposite direction to the particle itself. This generates a velocity difference between the particle's surface and the outside-edge of the interfacial double layer region, or viewed alternatively, a displacement of the particle relative to the bulk solution. Concentration gradients across a particle's interfacial region also result in a phoretic flow phenomenon termed diffusiophoresis.[11] An example of diffusiophoresis is observed when a gradient of electrolyte concentration is created across an initially even distribution of colloids. This causes the particles to migrate towards higher salt regions with a diffusion rate fifty times larger than that predicted by Brownian diffusion alone.[12] The discovery of these phoretic transport mechanisms leads to the suggestion that if an object could generate its own local field

Table 1 Significant micro scale swimming devices classified according to type, and in chronological order

A: Experimentally realised autonomous chemically powered swimmers

Swimmer	*Schematic/Micrograph*	*Dimensions*	*Catalyst*	*Fuel*	*Mechanisms*	*Swim in:*	*Max. Velocity*
(A1) Whitesides and co-workers[8]	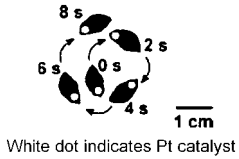	1 cm length	Pt	H_2O_2	Bubble propulsion	Aqueous meniscus	2 cm s^{-1}
(A2) Sen and co-workers[9]	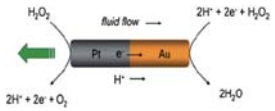	Diameter: 370 nm Length: 2 μm	Pt (+cathodic reactions at Au)	H_2O_2	Self electrophoresis/ Interfacial tension	Settled near boundary in aqueous solution	6.6 μm s^{-1}
(A3) Howse *et al.*[14]	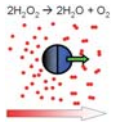	Diameter: 1.62 μm	Pt	H_2O_2	Pure self diffusiophoresis	Free aqueous solution	3 μm s^{-1}[a]
(A4) Mano and Heller[35]	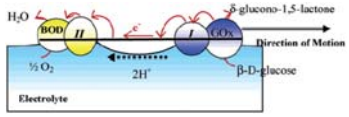	Diameter: 7 μm Length: 0.5–1 cm	Glucose oxidase and Biliruben oxidase	Glucose	Self electrophoresis	Aqueous meniscus	1 cm s^{-1}
(A5) Vicario *et al.*[37]	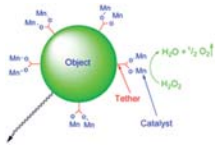	Diameter: 40–80 μm	Synthetic catalse	H_2O_2	Bubble/interfacial	Acetonitrile solution	35 μm s^{-1}
(A6) Wang *et al.*[23]	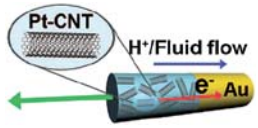	Diameter: 220 nm Length: 2 μm	Pt (CNT) (+cathodic reactions at Au)	H_2O_2/N_2H_4	Self electrophoresis	Settled near boundary in aqueous solution	>200 μm s^{-1}
(A7) Pantarotto *et al.*[36]	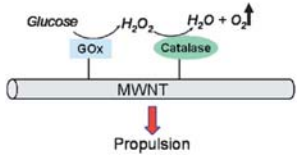	Diameter: 20–80 nm Length: 0.5–5 μm	Glucose oxidase and catalse	Glucose	Local oxygen bubble formation	Free aqueous buffer solution	0.2–0.8 cm s^{-1}

(A8) Gibbs and Zhao[21]	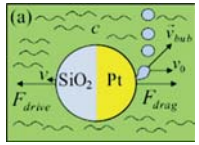	Diameter: 2 μm	Pt	H_2O_2	Bubble release mechanism	Aqueous solution	6 μm s^{-1}

B: Experimentally realised externally powered swimmers

Swimmer	*Schematic/Micrograph*	*Dimensions*	*Power source*	*Mechanism*	*Swim in:*	*Max. Velocity*
(B1) Dreyfus *et al.*[38]	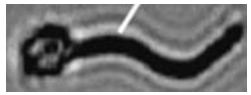	Length: 30 μm	External magnetic field	Flagella	Aqueous solution	Unkown
(B2) Tierno *et al.*[42]	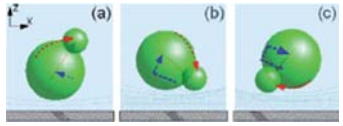	Diameters: 1: 2.8 μm 2: 1 μm	External magnetic field	Doublet rotation coupling with boundary interactions	Settled near boundary in aqueous solution	3.2 μm s^{-1}
(B3) Ghosh and Fischer[40]	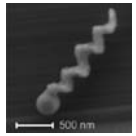	Length: 1–2 μm	External magnetic field	Propeller drive	Aqueous solution	40 μm s^{-1}

C: Theoretically predicted swimming mechanism[b]

Swimmer	*Schematic/Micrograph*	*Dimensions*	*Power source*	*Mechanism*	*Swims in:*
(C1) Najafi and Golestanian[5]	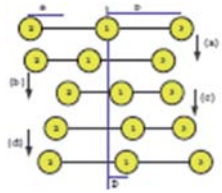	Micron scale	Theoretically, conformation changes in linking units	Time irreversible translations	Free solution

[a] This is a rigorously determined propulsion velocity solely due to the self-diffusiophoretic mechanism propelling the device. It should be noted velocities reported in other studies are averages of instantaneous frame-to-frame displacements, and so may include contributions due to Brownian motion. [b] The essential feature of this mechanism has recently been experimentally demonstrated for unconnected spheres using optical traps (44).

or concentration gradient within an otherwise homogeneous medium it would be able to move *via* "self-phoresis". While this effect has remained unproven in the original suggested context, as a plausible mechanism for moving cells,[11] self-phoresis has been used recently as the inspiration for designing a whole class of artificial micron scale swimming devices.

The feasibility of a self-generated concentration gradient propelling an object was initially demonstrated by the theoretical investigation of the fluid flows generated by a spherical particle with an asymmetric surface distribution of a catalyst able to decompose near by solute molecules.[13]

Inspired by this scheme, Howse *et al.* synthesised Janus particles (named after the two-faced Greek god) to verify the self-diffusiophoretic propulsion mechanism. The particles comprised a thin layer of platinum deposited on one side of spherical polystyrene beads (1.6 μm diameter), Table 1, A3.[14] Platinum was chosen due to its ability to catalytically decompose aqueous hydrogen peroxide solutions into oxygen and water, and so generate and maintain a concentration gradient in the interfacial region. The Janus particle trajectories were compared with equivalent pure polystyrene control spheres at different hydrogen peroxide concentrations, Fig. 1(a). From these plots it is apparent that asymmetric particles follow increasingly long paths and sample more of their surroundings in a given time period as hydrogen peroxide fuel concentration increases. Theory has been used to develop an equation to quantify the temporal evolution (Δt) of the mean-square displacements (ΔL^2) of such propelling Janus particles, in relation to their conventional Brownian diffusion coefficient (D), rotational time (τ_r) and velocity (V),

$$\Delta L^2 = 4D\Delta t + \frac{V^2\tau_r^2}{2}\left[\frac{2\Delta t}{\tau_r} + e^{-2\Delta t/\tau_r} - 1\right]$$

Analysis of this equation shows two expected temporal behaviours: for $\Delta t \ll \tau_r$ the limit of the equation becomes $\Delta L^2 = 4D\Delta t + V^2\Delta t^2$, introducing an additional quadratic term to the usual linear equation of Brownian motion, with an exponent corresponding to the square of the propulsion velocity; while for $\Delta t \gg \tau_r$ the limiting equation becomes $\Delta L^2 = (4D + V^2\tau_r)\Delta t$ reverting to linear behaviour, but with a new enhanced effective diffusion coeficient, $D_{eff} = 4D + V^2\tau_r$. This behaviour was indeed demonstrated by analysis of the mean-square displacement of the synthetic Janus particles, Fig. 1(b). Fitting the experimental data to this equation shows that self-diffusiophoresis results in an additional propulsion velocity of 3 μm s^{-1} at the maximum investigated fuel concentration (10% w/v hydrogen peroxide) corresponding to a thirty fold increase in the effective diffusion rate. While quantitative particle tracking has been limited to two-dimensions, particle movements relative to the microscope's focal plane suggests that the diffusion enhancement applied to all three-dimensions, consistent with the isotropic nature of the propulsion model.[15]

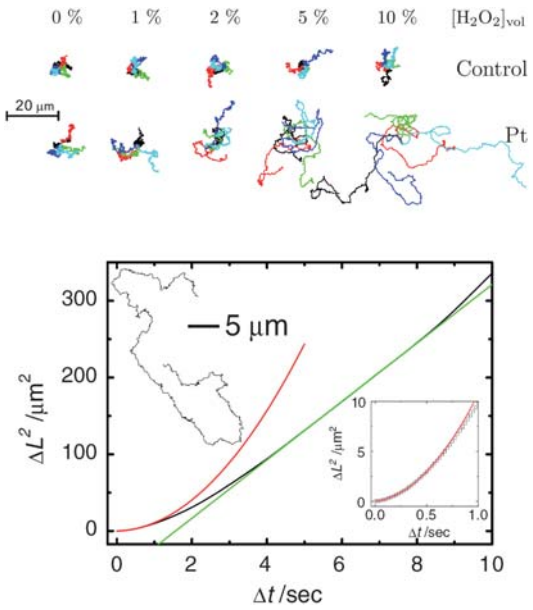

Fig. 1 (a) Trajectories of pure polystyrene control beads and hemispherically functionalised Pt beads as a function of hydrogen peroxide concentration. (b) Mean square displacement *versus* time plots for a platinum Janus particle swimming in a 10% w/v hydrogen peroxide solution together with the associated trajectory. A parabolic relationship is seen over short time scales ($<\tau_r$) due to directed runs. At longer time scales ($>\tau_r$) a linear, diffusive type relationship is re-established but with a much increased gradient due to super-diffusion resulting from the propulsive force. (From ref. 14.)

Two-dimensional trajectory analysis also reveals the Janus particles exhibit faster Brownian rotational diffusion at higher fuel concentrations, attributable to asymmetries in the platinum distribution across the coated side. This correlation partially suppresses the diffusion coefficient enhancement (*i.e.* particles change direction more often than they would do if Brownian rotation remained completely independent of the propulsion). As yet, the direction of the propulsive motion of the experimental Janus particles relative to the orientation of the asymmetric platinum coating, (*i.e.* if it moves towards or away from the interfacial catalytic decomposition product cloud) has not been unambiguously determined.

Since this experimental proof, the analysis used to predict the self-diffusiophoretic swimmer has been extended.[16] It turns out that the propulsive force and direction of a hemi-spherically heterogeneous swimmer will be affected both by the difference in catalytic activity of the two halves, and also by their surface mobilities. Similarly, numerical simulations of a dimer comprising a catalytically active sphere and an inert sphere show that the interaction of product and reagent "particles" with the inert sphere must differ for phoretic motion to occur, and that the relative interaction strength controls the direction of motion.[17] As surface mobility can be controlled by engineering nano-scale roughness and solvophobicity, this opens up the potential to design a range of swimmers exhibiting a variety of speeds and directions of motion.

While the self-diffusiophoresis model proposed above considers the interfacial region of the propelling particle, a more general model for osmotic motors, not limited to a boundary region limit has been developed.[18] This model suggests the maximum osmotic propulsion velocity for fast catalytic reactions is limited by the diffusive speed of the surrounding particles: if a swimmer moves faster than this it will leave the generated asymmetrical particle distribution behind and so lose the propulsive mechanism. Debate over the thermodynamics and

treatment of the solvent in this model has ensued.[19] One comment suggests the need to consider the exothermic nature of the chemical reaction driving the propulsion in this and other models. A clarification of many of these issues has been recently presented, re-asserting that no-net external force acts on a self-propelling particle and that the origin of propulsion for catalytic swimmers is due to self-generated phoretic effects rather than osmotic pressure.[20]

An alternative mechanism has been also been proposed to explain the motion of a silica analogue of the Janus particles described above, Table 1, A8.[21] The model suggests that small bubbles of oxygen form on the platinum coating, growing in size until they are eventually released, imparting momentum to the bead as they detach. This model was supported by trends in the silica Janus particles' swimming velocity as surface tension was varied using a surfactant. This bubble propulsion mechanism had previously been observed for Whitesides' millimetre scale hydrogen peroxide powered surface swimmers, which move away from oxygen bubbles generated by asymmetrical patterns of platinum.[8] While it is unclear if the gravity induced distortion of bubble shape invoked in the new bubble model is consistent with the isotropic propulsion seen for the polystyrene Janus particles, it is certain that the full investigation of all the mechanisms contributing to a given propulsion phenomenon will be essential to ensure that designed improvements to propelling materials are obtained efficiently.

2.2 Bi-metallic nanoswimming rods

The first reported autonomous nano-scale swimmers were solid bi-metallic rods consisting of a catalytically active segment such as platinum attached to an apparently inert material such as gold. These rods are the most widely investigated class of synthetic translators; however their geometry, combined with the possibility of a conductive path through the rod, has lead to debate about the propulsive mechanism.

2.2.1 Development of bi-metallic swimmers. The first studies of bi-metallic rods in the literature were reported almost simultaneously. Paxton *et al.* observed that gold-platinum rods with equal sized segments showed enhanced translations along their long axis at speeds of up to ten body lengths per second in the presence of hydrogen peroxide fuel, Table 1, A2.[9] Similarly, Bidoz *et al.* made gold-nickel rods (nickel will also catalyse peroxide decomposition), displaying powered rotational motions with the gold end attached to a silicon substrate.[10] Analysis of the motion of the translating gold/platinum rods showed that they achieved maximum average instantaneous speeds of up to 8 μm s^{-1}, and that this velocity increased with hydrogen peroxide fuel concentration up to 3% w/v. Unlike the spherical Janus particles discussed earlier, bimetallic rods displayed a significant increase in directionality as their velocity increased: their rotational diffusion was reduced by propulsion, Fig. 2. This effect is due to the asymmetrical drag forces experienced by rod-shaped objects. However, Brownian rotation is not entirely eliminated and rod trajectories viewed over long time-scales display enhanced diffusive behaviour rather than directed motion.

Although the design concept for these devices was to miniaturise Whitesides' millimetre scale bubble propelled swimmers,

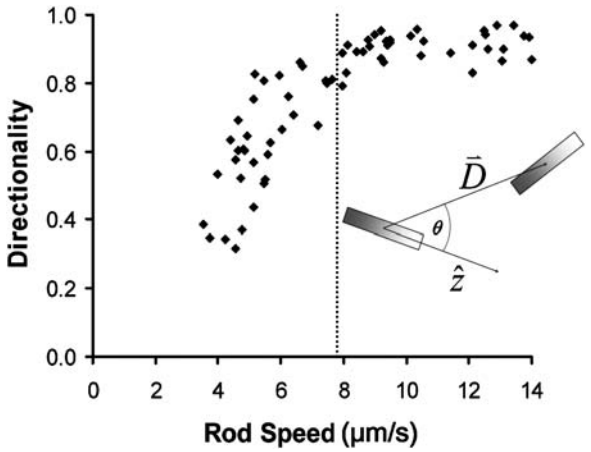

Fig. 2 Nano-rod motion can be analysed by calculating an average directionality parameter, defined as the cosine of the angle made between the rod's orientations in successive frames (inset). The relationship between directionality and speed is shown for 2 μm long platinum/gold rods in 3.3% w/v hydrogen peroxide solution. (From ref. 9.)

optical microscopy contradictorily revealed that gold-platinum rods travelled towards their platinum ends. This observation necessitated the development and investigation of alternative propulsion mechanisms. Early proposals included an interfacial tension model, suggesting that oxygen generated at the platinum catalyst produces a surface tension gradient along the rod due to solvent hydrogen bonding disruption,[9] and a Brownian ratchet mechanism where the evolved oxygen was thought to locally decrease viscosity to allow thermal driven directed motion.[22] However, recently an "electro-kinetic" model proposing that the rods move through a type of self-electrophoresis has gained experimental support. This mechanism considers the two rod segments as an interconnected electrochemical cell. At the platinum end anodic reactions occur during the catalytic surface oxidation of hydrogen peroxide to oxygen, generating protons in the interfacial solution region around the rod, and electrons in the rod itself. These reactions are coupled to the gold end which behaves as a cathode consuming the interfacial protons and received electron current during the reduction of hydrogen peroxide to water. The net effect of these coupled redox processes is to create a flow of protons in the rod's interfacial region from the platinum to the gold end. The proton flux in turn causes fluid motion in the same direction past the rod, or in the laboratory frame an observed translation of the rod towards the platinum end, Fig. 3.

A detailed investigation of the predictive power of this model was undertaken by measuring the half-cell potential of a variety of suitable nano-rod metals using ultramicroelectrodes immersed

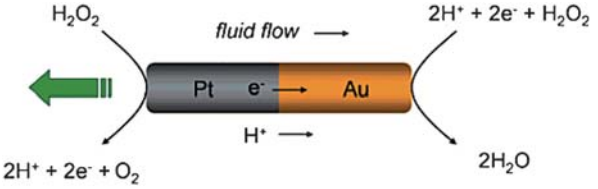

Fig. 3 A schematic illustrating self-electrophoresis (from ref. 24).

in hydrogen peroxide solutions as a near approximation to the actual swimming configuration.[23] Knowledge of these potentials allowed estimation of the likely magnitude and direction that any pair of metals used to make a rod would move in. These predictions were then compared to the observed motion of actual nano-rods made from the possible material combinations, with a high success rate. A further visual verification of the predicted direction of the fluid flow field in a coupled gold-platinum electrode system was obtained by monitoring tracer particles moving near to a gold-platinum catalytic micro pump.[24]

The possibility for additional phenomena contributing to nano-rod propulsion can not be ruled out.[25] For example, it is unclear how self-diffusiophoretic effects contribute. It is apparent that nano-rods produce an asymmetrical distribution of product particles in their interfacial region. A control experiment has been undertaken to investigate this using a non-conductive catalase rod segment in place of platinum to disable electrophoretic effects but retain the potential for self-diffusiophoresis; however only Brownian motion was detected.[23] Theory suggests that self-diffusiophoresis for rods is reduced by a factor of their aspect ratio relative to that of a sphere,[16] conversely the rods aspect ratio should aid detection of propulsion through their increased directionality.

Nano-rods are usually investigated in an electrostatically suspended state in close proximity to a boundary. The role that the nearby electric double layer of this boundary could play in effecting the proposed proton flow in the rod interfacial region, and the hydrodynamic benefits or penalties of phoretic swimming near a boundary have not to date been addressed. To our knowledge the three-dimensional behaviour of nano-rod propulsion has not been studied, as settling rates are very rapid for these dense objects. Studying conductive swimming devices in three-dimensions could help understand their swimming mechanism further, and will likely require the development of less dense analogues.

2.2.2 Faster moving nano-rods. Analysis of the energy conversion processes responsible for bi-metallic nano-rod motion reveals the original devices have low efficiency, and only convert a small amount of the energy produced in the driving catalytic reactions into motion.[25] However, recently the Wang group demonstrated modifications to the nano-rod composition that increase efficiency and propulsion speeds. The first improvement was obtained by mixing carbon nano-tubes into the platinum rod-end, Table 1, A6.[26] Pairing the composite rod segment with gold raised the average rod translation velocity to 43 μm s^{-1} in 5% w/v hydrogen peroxide solutions, Fig. 4. This strategy is based on carbon nano-tubes reported ability to improve electrocatalytic activity, resulting in an improvement in ease of hydrogen peroxide oxidation leading to a faster reaction rate and so more rapid electron transfer inside the nanorod. It was also noted that using a hydrazine/hydrogen peroxide fuel mix speeded rods up further to, on average, 93 μm s^{-1}, however with the resulting trajectories becoming predominantly circular. A small number of rods in this fuel mix were observed to travel at over 200 μm s^{-1}. Hydrazine was thought to enhance the catalytic rate of reaction at both parts of the rod and undergo efficient catalytic anodic decomposition itself. These improvements correspond to a three-hundred and fifty times increase in the power output of the nanorods compared to the original composition.

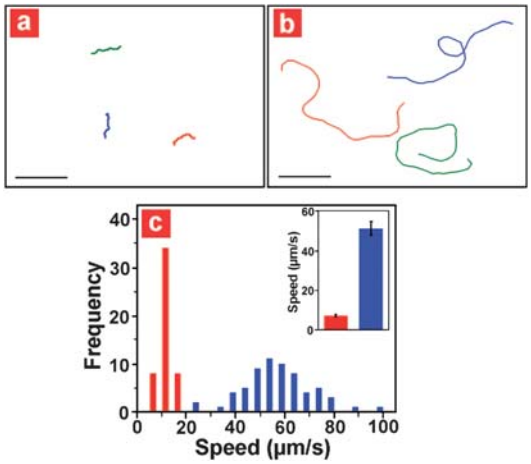

Fig. 4 (a) and (b) trajectories of conventional Pt anode and composite carbon nanotube/Pt anode rods respectively (c) comparison of speed distribution and average for the two rods (red – original; blue –CNT) (from ref. 26).

A second independent speed enhancement was achieved by changing composition at the cathodic rod end, by replacing pure gold with a silver-gold alloy.[27] The average rod speed increased with silver content up to an optimal composition (3 : 1 Ag : Au) producing an average translational speed of 110 μm s^{-1}. Further increases in silver content resulted in a sharp decline in velocity. This modification was based on previous Ag/Au alloys having been shown to enhance the electron transfer reactions of hydrogen peroxide. This speed increase is particulary straightforward to execute requiring only a simple adjustment to the plating bath composition during cathode deposition.

2.2.3 Controlling nano-rods. Despite differences in geometry and propulsion mechanism, all the swimmers discussed exhibit trajectories that are subject to random Brownian rotations, leading to propulsion manifesting itself as "super-diffusive" behaviour. However, to realise the envisaged nano-assemblers and biologically active nano-machines additional control of trajectory and speed is required, for example to move and dock an assembler with its cargo, or deliver a drug molecule to a specific biological target. To date this control has been achieved using two quite different methods. In the first, steering is achieved using external directing fields to damp the ubiquitous stochastic rotations allowing rods to be directed along linear paths. In addition, local environmental modifications can be used to alter the propulsion mechanisms efficiency, and so vary translation speed. A second, radically different method exploits emergent behaviour originating from the individually random trajectories to exert control over the statistical location of the swimming devices in analogy to biological processes such as chemotaxis.

2.2.3.1 External control of nano-rod direction and velocity. Directional control of self-propelling nano-rods was demonstrated by inserting additional magnetised segments into the rods and using external magnetic fields to establish an orientating and

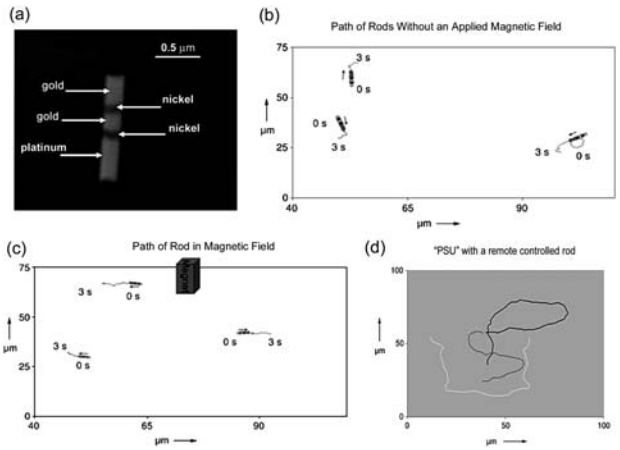

Fig. 5 (a) SEM image of a magnetically steerable rod. (b) and (c) The effect of applying an external magnetic field to the trajectory of the rods. (d) Demonstration of the manipulation of magnetic nano-rods to follow desired trajectories by changing the orientation of the external magnetic field (from ref. 28).

constraining magnetic torque.[28] It was found that the most effective rod structure was a "stripped" arrangement of short nickel single domain segments, allowing transverse magnetisation relative to the rod axis, Fig. 5(a). When a sufficiently strong external field was applied to a solution containing these magnetic-rods, the generated magnetic torque dominated the thermally induced orientation fluctuations and established alignment perpendicular to the field direction, Fig. 5 (b and c). This causes fuelled rods to propel along parallel linear trajectories. The applied field caused the rods to undergo unbiased rotation to the nearest perpendicular orientation, resulting in travel in both directions relative to the field according to the random distribution of the rods' orientation at the moment the field was applied. Analysing the linear propulsion speeds proved that the orientating field did not affect the propulsion mechanism, demonstrating that independent direction control of nano-rods is possible without retarding velocities. Changing the magnetic field orientation also allowed the rods to be steered along desired trajectories, with a reasonable degree of control, Fig. 5(d). The magnetic alignment method has also been used to orientate the faster moving composite platinum–carbon nanotube nano-rods. This allowed a visual comparison of the effect of nano-rod composition and fuel type on linear velocity, by staging nano-races, Fig. 6.

In addition to directional control, it is possible to speed up and slow down nano-rods. One example utilised a thermal pulse generated by heating a wire to cause a local increase in solution

Fig. 6 Nanomotor racing. Optical microscopy images with tracked lines showing the sped of Au/Ni/Au/Pt (a) and (d) and Au/Ni/Au/Pt-CNT (b, c) nanomotors magnetically orientated in 2.5% wt hydrogen peroxide with (c, d) and without (a, b) hydrazine at 0.15% wt (fromref. 26).

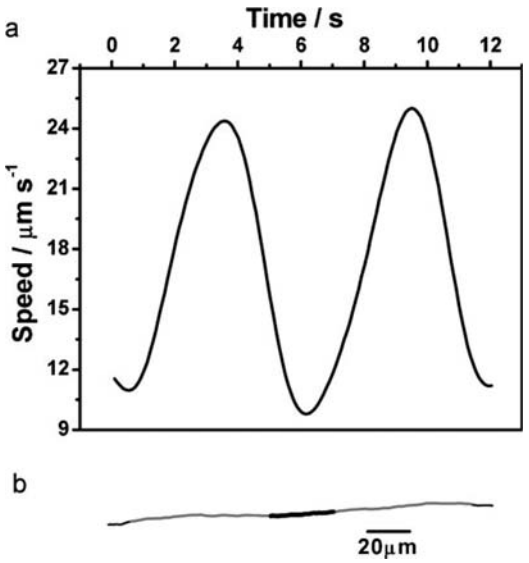

Fig. 7 Demonstration of thermal pulse acceleration and deceleration of a magnetically confined nano-rod. (a) Graph of speed *versus* time (b) Trajectory, with distances travelled during (light grey) and in between (dark grey) the evenly spaced thermal pulses. (From 29).

temperature (up to 65 °C) and a corresponding temporary increase in rod average speed (from 14 μm s^{-1} to 45 μm s^{-1}).[29] Thermally induced acceleration was thought to be caused by activation of the electrochemical reactions that drive self-electrophoresis, although a corresponding reduction in water viscosity at the higher temperatures may also contribute. It was also shown that a thermal pulse could cause acceleration and deceleration of a magnetically orientated swimmer confined to a linear trajectory, Fig. 7. A second method to achieve speed control installed an electrode in close proximity to the nano-rods to enable electrochemical modification of the swimming solution.[30] The induced changes in the solution composition in turn effected the redox reactions driving propulsion. A complex relationship between the applied voltage step size and direction and the measured average rod speed was reported, however it was shown to be possible to cause repeated cyclical rod acceleration and deceleration using an appropriate electrode voltage program. It was suggested that this effect was mainly due to changes in solution oxygen concentration caused by the electrode. A degree of speed control was also demonstrated to be possible for magnetic nickel segmented rods. By using a rapid manipulation of the external magnetic field it was possible to induce rods to execute brief "stop-turn-and-go" manoeuvres.[31]

2.2.3.2 Emergent behaviour. Directing nano-rod "traffic" using external fields is a large step towards exploiting propulsive devices for small scale directed assembly and transport. However, in other situations devices will need to autonomously move towards a particular chemical "signal", for example secretions from a cell to deliver a targeted drug cargo. In nature, the ability to move up or down chemical gradients is termed chemotaxis, and is demonstrated by bacteria using the run and tumble method. This requires the moving bacteria to employ temporal sensing of chemical signal molecules and so respond to local concentrations. A sensed increase in the chemical signal

results in a slower tumbling rate and *vice versa*. Results obtained by Sen's group have shown that an analogue of this process can emerge statistically for nano-rods placed in a gradient of hydrogen peroxide fuel,[32] however in this case rods are unable to sense the local fuel concentration. Two experimental set-ups were used to demonstrate statistical up-fuel gradient propulsive nano-rod accumulation. In the first a gel loaded with a high concentration of hydrogen peroxide established the gradient. Over a period of four and a half days 70% of the nanorods accumulated around the hydrogen peroxide leaching gel, Fig. 8 (a). The second demonstration used capillary tubes to separate reservoirs of various hydrogen peroxide concentrations, from nano-rods swimming in water. Optical microscopy showed that rods accumulated at the capillary ends with a number density corresponding to the fuel concentration in the capillary. In this example, the rods had to leave their usual sedimented electrostatic suspended state and climb up a distance corresponding to the thickness of the capillary glass (150 μm) to reach their target. To establish that these phenomena were not caused by straightforward colloidal diffusiophoresis,[12] the gel experiment was repeated with a monometallic pure gold control rod, which did not show the same propensity to accumulate near the fuel source. This observation suggested that the propulsive mechanism played a part in the observed statistical migration. The behaviour has been qualitatively visualised as the rods random walk leading to them spending equal times moving up and down the fuel gradient, but as they travel further during their "upstream" excursions (due to the relationship between velocity and hydrogen peroxide concentration) a bias towards statistical migration is established.

Sen's group has shown other examples of collective behaviour originating from the interactions of particles undergoing self-phoretic propulsion.[33] In a system comprising micrometre sized silver chloride particles, ultra-violet irradiation light initiated photochemical reactions releasing ionic species with differential diffusion rates (H^+ and Cl^-). The resulting ionic separation created an electric field causing the silver chloride particles to show enhanced phoretic motion. At a sufficiently high particle density, the enhanced motion was accompanied by an observed tendency for the particles to form agglomerates. This clumping behaviour was thought to be due to interactions between the particles self-generated photochemically induced ion gradient. Inactive silica particles mixed into this system were also found to surround the photolytic particles during irradiation, suggesting they responded to the ion-field generated by diffusiophoresis, Fig. 8 (b). These observations suggest ionic signalling can produce complex self-organised structures. An interesting photo-patterning effect was also reported during the localised illumination of a solution containing silver on silica Janus particles. In dilute hydrogen peroxide solutions, ultra-violet irradiation initiated photolysis at the silver surface to produce differentially mobile Ag^+ and OOH^- ions, resulting in phoretic motion. If the illumination was performed locally through a microscope objective, a macroscopic gradient of these ions is produced due to variations in the incident photon flux. This gradient caused a statistical movement of the Janus particles away from the irradiated region, demonstrating negative phototaxis, Fig. 8(c). In line with all the experiments discussed in this section, a critical particle density was required for this effect to be observed.

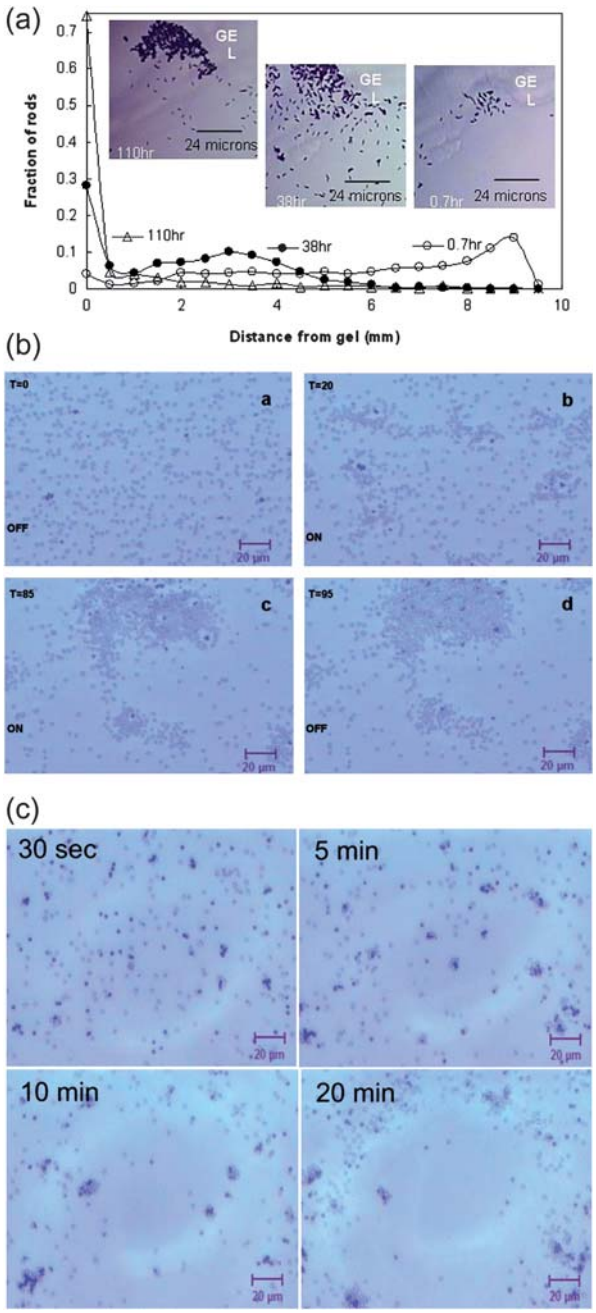

Fig. 8 (a) Micrographs showing the accumulation of nano-rods near a hydrogen peroxide soaked gel positioned near the top left corner of the image, overlaid on corresponding rod distribution profiles (from ref. 32). (b) Silica particles aggregate around the darker and larger silver chloride particles during UV irradiation (from ref. 33). (c) Silver on silica janus particles undergo negative phototaxis away from a centrally irradiated region (from ref. 33).

2.2.4 Cargo transport. Various demonstrations of propelling nano-rods towing or pushing passive cargos have been reported. In one example, gold-platnium nano-rods were coupled to polymeric "bead" cargo using either electrostatic interactions or streptavidin-biotin binding.[34] The bead cargo increased the drag force on the nano-rod motor, resulting in a decrease in overall propulsion velocity compared to an unburdened rod. For

example a rod pulling a 2 μm diameter bead travelled at 3.5 μm s^{-1}, compared to a 9 μm s^{-1} free swimming velocity. Drag increased as a function of cargo diameter, and when bead diameters reached 3.5 μm no propulsion was detected. Analysis suggested that the speed reduction was solely due to additional drag rather than a disruption of the nano-rods propulsion mechanism. Bead laden rods also showed different rotational behaviour with biased rotations commonly induced due to asymmetric attachment. However magnetic nano-rods coupled to bead cargo could be controlled by external fields to achieve directed movement, with a few degrees wobble, Fig. 9. Bead laden nano-rods were also shown to exhibit statistical migration up a hydrogen peroxide fuel gradient.[34]

Composite carbon-nanotube/platinum-gold rods were also used to transport cargo inside microfluidic channels.[31] Confining the rod to channels allowed them to be easily directed to follow complex paths using external magnetic guidance. However, confinement reduced their swimming speeds, possibly due to channel materials absorbing hydrogen peroxide fuel as suggested in the study. Despite operating at reduced power, these rods were able to transport a magnetically attached 1.3 μm diameter iron particle at 9 μm s^{-1}, and move particles with diameters up to 4 μm. Magnetic cargo attachment combined with magnetic steering allowed "en-route" loading. The external steering magnetic field could also be used to cause the rod-cargo ensemble to execute a sudden sharp u-turn, resulting in the cargos "slingshot" release. This arrangement allowed a complete "load, drag and drop" cycle of cargo manipulation, Fig. 10.

3. Alternative power sources for chemical swimmers

The majority of artificial swimming devices have been powered using the catalytic reduction of hydrogen peroxide solutions at a metallic surface. However, to extend the range of environments accessible by these devices alternative fuel sources and catalysts are required. For example, biologically active swimmers will ideally be powered by ubiquitous bio-molecules. To address this, two related studies have shown the possibility of using coupled enzymatic reactions to propel carbon fibres, and single wall nano-tubes using glucose as fuel. In the first case opposite ends of the conducting fibre were functionalised with glucose oxidase and bilirubin oxidase, the former capable of oxidising glucose, and the latter a biocatalyst for a four-electron reduction of oxygen to water, Table 1, A4.[35] This established a glucose fuelled redox reaction along the fibre, which in turn produced a proton flux in the fluid providing a bio-chemically powered propulsive mechanism analogous to nano-rod self-electrophoresis. These fibres were observed to move with velocities up to 1 cm s^{-1} as long as they were sufficiently hydrophobic to remain at the meniscus; viscous drag being too strong for submerged propulsion. Fibre trajectory was dependant on the relative loadings of the two enzymes. If the two functionalised ends of the fibre were insulated from each other the propulsion stopped, supporting an electrochemical mechanism. A similar arrangement, on a smaller length scale was established by functionalising a multi-wall carbon nanotube with glucose oxidase and catalase, Table 1, A7.[36] In this case glucose oxidase converts glucose to hydrogen peroxide, which can in turn be catalytically decomposed by catalase. This provides a potential route for the device to generate its own peroxide fuel from glucose. These devices were observed to propel when suspended in glucose solutions. As free solution mixing of this enzyme combination was known to cause oxygen depletion, this was the predicted propulsion mechanism, however in fact the enzyme combination functioned differently when localised on the nano-tube and oxygen bubbles were created on the fibres, suggesting bubble propulsion.

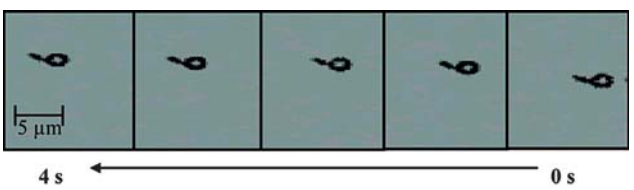

Fig. 9 A magnetically orientated nano-rod motor pulls its bead cargo (from ref. 34).

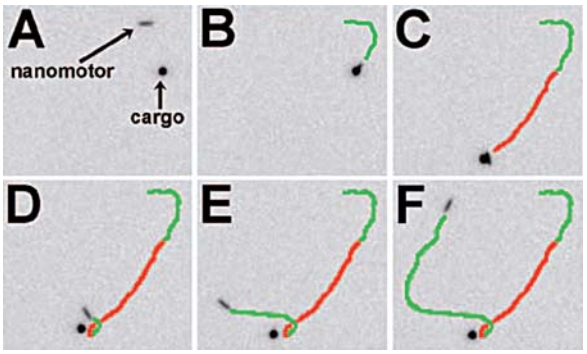

Fig. 10 Sequential optical microscopy images of an en-route cargo pickup, transport, and release. Green and red traces show the path travelled by the rod and cargo loaded rod respectively (A, B) manipulation and pick up (C) transport (D) release (E + F) continued rod motion after release (from ref. 31).

A separate study has suggested that synthetic analogues of biocatalysts may be used to power nano-swimming devices. This potentially allows fine tuning of features of the molecular power source, for example; activity, attachment chemistry, and tethering length. To demonstrate this approach, covalent imine coupling was used to attach synthetic catalase to amino-propyl modified silica beads (diameter 40–80 μm) Table 1, A5.[37] These beads were observed to decompose hydrogen peroxide, and underwent propulsion correlating to oxygen bubble generation. No attempt to induce heterogeneous catalyst coverage was made, instead it was thought that asymmetries in the beads surface produced unevenly distributed bubble nucleation points, leading to the beads translation, and in some cases rotation.

4. Nature inspired swimming mechanisms

Nature and theoretical modelling suggest alternative non-phoretic based swimming mechanisms. For example, rotating or wave propagating flagella are commonly used to move cells in biological systems; while simple arrangements of translating spheres have had their theoretical swimming properties widely demonstrated.[5] Despite this, to date the later system has only been experimentally realised in a highly abstracted form, and synthetic e.g flagellar swimmers and analogues can only be

caused to move using external fields. This illustrates the real barrier for producing autonomous synthetic analogues of these swimming mechanisms: the extreme difficulty in designing onboard molecular power sources with the output, size and efficiency needed to actuate the required rotational and translational motions. However, despite this current limitation, examples of micron scale externally powered devices are discussed, to allow comparison of their potential applications and effectiveness with the existing catalytic translators discussed above.

The first demonstration of synthetic micro swimming flagella was produced by Dreyfus *et al.*[38] They demonstrated the spermatozoa like motion of a string of magnetic particles attached to a red blood cell, Table 1, B1. Flexible linkage of the bead chain was achieved using DNA strands functionalised with Biotin at either end binding to a Streptavidin coating on the magnetic beads. The combination of a static magnetic field to orientate the swimming chain, and a sinusoidal field to generate non-time reversible wave propagation down the filament, dragged the attached red-blood cell in a tail first configuration. Similar moving structures have also been produced spontaneously by the applied magnetic field induced self-assembly of magnetic beads at a liquid surface.[39] Cork-screw shaped artificial swimmers have also been fabricated and shown to be able to be controlled in similar ways to the nano-rods described above, Table 1, B3.[40] When these structures were caused to rotate using an applied homogenous field, the helical propeller produced translations up to a speed of 40 μm s^{-1}. By adjusting the field direction, accurate trajectory control was demonstrated, and the propellers were shown to be able to push a 5 μm diameter bead. In a related example, pitch control was used to prevent a similar propeller system sedimenting under gravity, illustrating that these devices are also capable of sustained free solution swimming.[41]

An additional original swimming mechanism has been recently demonstrated by Tierno *et al.*[42,43] A doublet of two differently sized paramagnetic doped polystyrene beads, bound using short chains of DNA, Table 1, B2, is caused to rotate by an external magnetic field, in proximity to a solid interface. Interactions between the doublet and the boundary break the otherwise time-reversible motion to result in directed motion. It should be noted that the swimming mechanism relies on the doublet being in a suspended state in close proximity to the bounding containers wall, and would not produce motion in free solution. The velocity achieved by this doublet is 3 μm s^{-1}, and the doublet can be driven around a desired path in a microfluidic channel by switching the actuating magnetic fields' direction.

Many more swimming designs are proving difficult to realise experimentally. For example the apparently simple three-sphere swimmer requires a specific order of non-time reversible expansions and contractions from two linking components, Table 1, C1. Although proof of concept for this arrangement has been recently experimentally demonstrated using unconnected beads in optical traps,[44] this approach needs more development to produce an autonomous swimmer. Promisingly, a recent study presents details of a conformational change based driving mechanism that at least provides a starting point for generating the necessary displacements in a physically linked device.[45] As a final note it is mentioned that the famous restriction imposed on low Reynolds number swimming requiring non-time reversible deformations has been shown to break down in simulations of swarms of interacting swimmers, potentially allowing very straightforward translators to generate cooperative fluid motion.[46,47] Such efforts, combined with the development of small scale components capable of converting chemical energy into motion that will enable autonomous swimming using powered translations to become reality.

5. Conclusions and future directions

As a result of work by several research groups, bi-metallic nano-rod systems have reached the proof-of concept stage for many nanoscale applications. Magnetically steered nano-rods are able to shuttle cargo with a degree of spatial control in fluid environments. Intrinsic rod velocities can be varied as required by compositional and fuel changes, up to an impressive top speed of 200 μm s^{-1}. Additional online speed control is possible using local environment modifications. Furthermore the ability to switch the path of nano-rods at micro fluidic channels junctions allows the sorting and separation of components. The next stages of nano-rod development will likely focus on improving the autonomy of assembly processes. For example, the potential for nano-rods to show specificity for a particular type of cargo could be achieved using selective attachment chemistry. Furthermore harnessing the complex behaviour of interacting phoretic devices potentially provides another mechanism for generating complicated ordered structures with little external intervention.

The two-sphere swimmer developed by Tierno, also exhibits a similar ability to translate around controlled paths in micro fluidic devices, however requires external power as well as direction, and has not yet been coupled to cargo. The miniaturised helical propeller devices also have similar potential utility to nano-rods, but again require external actuation.

However, some key problems still remain for biological transport applications such as targeted drug delivery, and it is suggested that *in vivo* nano-scale transporters will need to combine features from a variety of the swimming systems discussed above. For example, while nano-rods propensity to swim in two dimensions after sedimenting is beneficial for assembly applications, in biological systems it is likely that useful swimmers will be more neutrally buoyant and able to swim and track down delivery targets in three-dimensions. Three-dimensional diffusive propulsion has been observed for the neutrally buoyant platinum on polystyrene Janus particles, however this system shows lower propulsion speeds compared to nano-rods.

Another requirement is to use a biologically common fuel source. Reports of two enzyme powered glucose fuelled carbon based swimmers is promising in this respect, although the propulsion mechanism is based on current flow, and was shown to diminish at high salt concentrations. This appears to be a general problem for the phoretic propulsion mechanism in biological high-salt environments, although it has been recently suggested that carbon-nanotube/platinum anodic enhancement may overcome this limitation.[48] As for achieving directional control *in vivo*, this is likely to rely on an autonomous chemical gradient sensing mechanism, such as the reported statistical chemotaxis. However at present this only results in very slow statistical movements of propelling devices.

As mentioned above, flagella swimming is used to solve transport problems at the scales of interest in nature. It is instructive to consider if this, or other theoretically proposed swimming mechanisms, have intrinsic advantages over catalytic propulsion. From the above descriptions of artificial flagella swimmers and propeller driven devices it appears that they display similar propulsive performance to the catalytic systems in terms of translation speed and cargo moving power, and indeed the fastest catalytic devices exceed the speeds achieved by biological flagella propulsion. In addition, flagellae or three-spheres and related models do not display obvious advantages in effecting directional control. One possible advantage of translationally powered devices is they exhibit more potential to be self-contained entities, whereas an intrinsic part of the mechanism for catalytic swimming is to carry out chemical reactions on exposed surfaces and secrete chemical reaction products.

Given the difficulties in generating synthetic motion, and in particular designing power sources for translational devices, harvesting existing working biological motor and propulsion systems for integration into man-made devices provides an alternative strategy. For example flagella driven bacteria have generated propulsion when attached asymmetrically to a colloidal bead.[49] Delicate harvesting of the actual motors that drive flagellae rotations has also been used to drive man-made mechanical parts.[50,51] While this approach has the potential to provide the sought after efficient motor components for nano-swimmer devices, the harvested components are relatively unstable, showing short active life-times, and requiring careful handling, although have the advantage of being able to function in the biological environmental.

While this review has considered the utility of nano-swimmers for two demanding nano-technological transport problems, it should finally be noted that a large range of additional applications have been enabled by the development of swimming devices. For example, nanorods have been used to make novel measurements at liquid interfaces[22] and in the bulk[52] while unregulated super-diffusion has the potential to drive enhanced fluidic mixing rates. As nano-swimmer development continues towards the ultimate nano-transport goals it is certain that a whole host of interesting phenomena and devices will emerge along the way.

Acknowledgements

SE and JRH acknowledge EPSRC (EP/G04077X/1) for funding.

References

1 Z. Ghalanbor, S. A. Mareshi and B. Ranhbar, *Med. Hypotheses*, 2005, **65**(1), 198.
2 E. M. Purcell, *Am. J. Phys.*, 1977, **45**, 3.
3 M. Schliwa and G. Woehlke, *Nature*, 2003, **422**, 759.
4 R. Lipowsky, Y. Chai, S. Klumpp, S. Leipelt and M. J. I. Muller, *Phys. A*, 2006, **372**, 34.
5 A. Najafi and R. Golestanian, *J. Phys.: Condens. Matter*, 2005, **17**, S1203.
6 R. A. L. Jones, *Soft Machines*, Oxford University Press, Oxford, 2004.
7 J.-H. Cho, C. S. Lin, C. D. Richards, R. F. Richards, J. Ahn and P. D. Ronney, *Proc. Combust. Inst.*, 2009, **32**, 3099.
8 R. F. Ismagilov, A. Schwartz, N. Bowden and G. M. Whitesides, *Angew. Chem., Int. Ed.*, 2002, **41**, 652.
9 W. F. Paxton, K. C. Kistler, C. C. Olmeda, A. Sen, S. K. St. Angelo, Y. Cao, T. E. Mallouk, P. E. Lammert and V. H. Crespi, *J. Am. Chem. Soc.*, 2004, **126**, 13424.
10 S. Fournier-Bidoz, A. C. Arsenult, I. Manners and G. A. Ozin, *Chem. Commun.*, 2005, 441.
11 J. L. Anderson, *Annu. Rev. Fluid Mech.*, 1989, **21**, 61.
12 J. P. Ebel and J. L. Anderson, *Langmuir*, 1988, **4**, 396.
13 R. Golestanian, T. B. Liverpool and A. Ajdari, *Phys. Rev. Lett.*, 2005, **94**, 220801.
14 J. R. Howse, R. A. L. Jones, A. J. Ryan, T. Gough, R. Vafabakhsh and R. Golestanian, *Phys. Rev. Lett.*, 2007, **99**, 048102.
15 Unpublished data: Pt-PS Janus particles are observed to sink in pure water due to their negative buoyancy as evidenced by the need to slowly lower the microscopes objective to retain focus during tracking. However, at high hydrogen peroxide concentrations (5 and 10%) additional rapid focus corrections are required both "up" and "down" to retain particle focus, indicating that the particle is undergoing additional displacements in the vertical direction.
16 R. Golestanian, T. B. Liverpool and A. Ajdari, *New J. Phys.*, 2007, **9**, 126.
17 G. Rückner and R. Kapral, *Phys. Rev. Lett.*, 2007, **98**, 150603.
18 U. M. Cordova-Figueroa and J. F. Brady, *Phys. Rev. Lett.*, 2008, **100**, 158303.
19 T. M. Fischer and P. Dhar, *Phys. Rev. Lett.*, 2009, **102**, 159801; U. M. Cordova-Figueroa and J. F. Brady, *Phys. Rev. Lett.*, 2009, **102**, 159802; F. Julicher and J. Prost, *Phys. Rev. Lett.*, 2009, **103**, 079801; U. M. Cordova-Figueroa and J. F. Brady, *Phys. Rev. Lett.*, 2009, **103**, 079802.
20 F. Jülicher and J. Prost, *Eur. Phys. J.*, 2009, **29**, 27.
21 J. G. Gibbs and Y. –P. Zhao, *Appl. Phys. Lett.*, 2009, **94**, 163104.
22 P. Dhar, Th, M. Fischer, Y. Wang, T. E. Mallouk, W. F. Paxton and A. Sen, *Nano Lett.*, 2006, **6**, 66–72.
23 Y. Wang, R. M. Hernandez, D. J. Bartlett, Jr., J. M. Bingham, T. R. Kline, A. Sen and T. E. Mallouk, *Langmuir*, 2006, **22**, 10451.
24 W. F. Paxton, P. T. Baker, T. R. Kline, Y. Wang, T. E. Mallouk and A. Sen, *J. Am. Chem. Soc.*, 2006, **128**, 14881.
25 W. F. Paxton, A. Sen and T. E. Mallouk, *Chem.–Eur. J.*, 2005, **11**, 6462.
26 R. Laocharoensuk, J. Burdick and J. Wang, *ACS Nano*, 2008, **2**(5), 1069.
27 U. K. Demirok, R. Laocharoensuk, K. M. Manesh and J. Wang, *Angew. Chem., Int. Ed.*, 2008, **47**, 9349.
28 T. R. Kline, W. F. Paxton, T. E. Mallouk and A. Sen, *Angew. Chem., Int. Ed.*, 2005, **44**, 744–746.
29 S. Balasubramanian, D. Kagan, K. M. Manesh, P. Calvo-Marzal, G.-U. Fleschig and J. Wang, *Small*, 2009, **5**(13), 1569.
30 P. Calvo-Marzal, K. M. Manesh, D. Kagan, S. Balasubramanian, M. Cardona, G.-U. Flechsig, J. Posner and J. Wang, *Chem. Commun.*, 2009, 4509.
31 J. Burdick, R. Laocharoensuk, P. M. Wheat, J. D. Posner and J. Wang, *J. Am. Chem. Soc.*, 2008, **130**, 8164.
32 Y. Hong, N. M. K. Blackman, N. D. Kopp, A. Sen and D. Velegol, *Phys. Rev. Lett.*, 2007, **99**, 178103.
33 A. Sen, M. Ibele, Y. Hong and D. Velegol, *Faraday Discuss.*, 2009, **143**, 15.
34 S. Sundararajan, P. E. Lammert, A. W. Zudans, V. H. Crespi and A. Sen, *Nano Lett.*, 2008, **8**(5), 1271.
35 N. Mano and A. Heller, *J. Am. Chem. Soc.*, 2005, **127**, 11574.
36 D. Pantarotto, W. R. Browne and B. L. Feringa, *Chem. Commun.*, 2008, 1533.
37 J. Vicario, R. Eelkema, W. R. Browne, A. Meetsama, R. M. La Crois and B. L. Feringa, *Chem. Commun.*, 2005, 3936.
38 R. Dreyfus, J. Baudry, M. L. Roper, M. Fermigier, H. A. Stone and J. Bibette, *Nature*, 2005, **437**, 862.
39 A. Snezhko, M. Belkin, I. S. Aranson and W.-K. Kwok, *Phys. Rev. Lett.*, 2009, **102**, 118103.
40 A. Ghosh and P. Fischer, *Nano Lett.*, 2009, **9**(6), 2243.
41 L. Zhang, J. J. Abbott, L. Dong, B. E. Kratochvil, D. Bell and B. J. Nelson, *Appl. Phys. Lett.*, 2009, **94**, 064107.
42 P. Tierno, R. Golestanian, I. Pagonabarraga and F. Sagues, *J. Phys. Chem. B*, 2008, **112**, 16525.
43 P. Tierno, R. Golestanian, I. Pagonabarraga and F. Sagues, *Phys. Rev. Lett.*, 2008, **101**, 218304.
44 M. Leoni, J. Kotar, B. Bassetti, P. Cicuta and M. C. Lagomarsion, *Soft Matter*, 2009, **5**, 472.

45 R. Golestanian and A. Ajdari, *Phys. Rev. Lett.*, 2008, **100**, 038101.
46 E. Lauga and D. Bartolo, *Phys. Rev. E: Stat., Nonlinear, Soft Matter Phys.*, 2008, **78**, 030901.
47 G. Alexander and J. M. Yeomans, *Europhys. Lett.*, 2008, **83**, 34006.
48 Preliminary data mentioned but not shown in ref. 19.
49 B. Behkam and M. Sitti, *Appl. Phys. Lett.*, 2008, **93**, 223901.
50 R. K. Soong, G. D. Backand, X. Xu, L. Huang and C. A. Mirkin, *Science*, 2000, **290**, 1555.
51 M. G. L. Van den Heuvel and C. Dekker, *Science*, 2007, **317**, 333.
52 D. Kagan, P. Calvo-Marzal, S. Balasubramanian, S. Sarrayasamitsathit, K. M. Manesh, G.-U. Flechsig and J. Wang, *J. Am. Chem. Soc.*, 2009, **131**, 12082–12083.

